NASA CONTRACTOR REPORT

NASA CR-2000

DYNAMIC RESPONSE OF HIGH-FREQUENCY PRESSURE TRANSDUCERS TO LARGE AMPLITUDE SINUSOIDAL PRESSURE OSCILLATIONS

by Richard E. Robinson

Prepared by
BATTELLE
Columbus, Ohio 43201
for Lewis Research Center

NATIONAL AERONAUTICS AND SPACE ADMINISTRATION • WASHINGTON, D. C. • APRIL 1972

1. Report No.	2. Government Accession No.	3. Recipient's Catalog No.
CR-2000		

4. Title and Subtitle	5. Report Date
DYNAMIC RESPONSE OF HIGH-FREQUENCY PRESSURE TRANSDUCERS TO LARGE AMPLITUDE SINUSOIDAL PRESSURE OSCILLATIONS	April 1972
	6. Performing Organization Code
7. Author(s)	8. Performing Organization Report No.
Richard E. Robinson	None
	10. Work Unit No.
9. Performing Organization Name and Address	
Battelle 505 King Avenue Columbus, Ohio 43201	11. Contract or Grant No. NAS 3-11229
	13. Type of Report and Period Covered
12. Sponsoring Agency Name and Address	Contractor Report
National Aeronautics and Space Administration Washington, D.C. 20546	14. Sponsoring Agency Code

15. Supplementary Notes

Project Manager, Richard J. Priem, Chemical Propulsion Division, Technical Monitor, Marshall C. Burrows, Physics and Chemistry Division, both of NASA Lewis Research Center, Cleveland, Ohio

16. Abstract

Dynamic response characteristics of six currently used dynamic pressure transducers were investigated by using a large-amplitude sinusoidal-pressure generator. Frequencies between 1 and 15 kilohertz with corresponding peak-to-peak pressure-oscillation amplitudes ranging between 73 and 8 percent of bias pressure and bias pressures between 15 and 300 psia (10-207 N/cm^2 abs) were utilized. Amplitude-ratio data as functions of frequency and pressure level are given for all transducers. The generator design and performance and associated instrumentation are described.

1. Pressure Sensors
2. Dynamic Response

17. Key Words (Suggested by Author(s))	18. Distribution Statement
Pressure transducers Transducer calibration Dynamic response	Unclassified - unlimited

19. Security Classif. (of this report)	20. Security Classif. (of this page)	21. No. of Pages	22. Price*
Unclassified	Unclassified	34	$3.00

* For sale by the National Technical Information Service, Springfield, Virginia 22151

DYNAMIC RESPONSE OF HIGH-FREQUENCY PRESSURE TRANSDUCERS TO LARGE AMPLITUDE SINUSOIDAL PRESSURE OSCILLATIONS

by Richard E. Robinson

SUMMARY

Dynamic response characteristics of six pressure transducers, representative of those most current and frequently used, were investigated. Amplitude ratios as functions of frequency and bias pressure were determined using a large amplitude sinusoidal pressure generator. Frequencies between 1 and 15 kilohertz with corresponding peak-to-peak pressure oscillation amplitudes ranging between 73 and 8 percent of bias pressure and bias pressures between 15 and 300 pounds per square inch absolute (10 and 207 neutons per square centimeter absolute) were utilized. Effects of transducer type and manufacturer, protective passages, coolants, and diaphram coating were also studied. Descriptions of the generator, its operating characteristics, and the instrumentation used to measure frequency and amplitude ratio are given.

INTRODUCTION

The need to measure "nonsteady" pressure has existed for many years and recent developments have increased the requirements for and the complexities of these measurements. Protection from severe environments and space limitations have added further complexities requiring transducers with devices such as probes, cavities, coolant bleeds, and coatings. The dynamic calibration of a pressure transducer can ideally be accomplished by sensing known inputs from a periodic pressure generator at known frequencies and amplitudes. The observed response, including the magnitude, waveform, and phase lag, can then be compared with the known input at various conditions. Calibration with only one frequency at a time for accuracy and simplicity can be accomplished with a sinusoidal pressure generator (SPG). (1, 2, 3)*

This report summarizes the dynamic frequency response characteristics of six frequently used, current, dynamic pressure transducers. Transducer dynamic response characteristics in the form of amplitude ratio were investigated with an inlet-modulated SPG on each type of transducer selected.

---

* Numbers in parentheses refer to references listed at the end of this report.

TEST APPARATUS AND PROCEDURE

Generator

The design concept of the sinusoidal pressure generator, an inlet-modulated, gas-flow-through device (IM-SPG), is shown in Figure 1, and detailed description of the generator is given in references (2) and (3). Pressure oscillations are produced with this type of generator by changing the mass content in a chamber, i.e. controlling the gas flow into and out of the chamber. The oscillating or sinusoidally varying static pressure in the chamber is used to dynamically calibrate pressure transducers. The pressure in the chamber is sensed by the flush-mounted test transducer and by a flush-mounted reference or standard transducer.

Basically, the generator consists of a cylindrical chamber with a modulated inlet flow opening and a fixed outlet flow opening (See Figure 1). The chamber dimensions are 0.75 inch (1.91 cm) in diameter and 0.262 inch (0.665 cm) in length. The chamber is filled with several types of porous materials (acoustic absorbing filler). This filler improves pressure wave shape by reducing chamber harmonics and flow turbulence (which excites transducer resonances (3)). The two flow openings are placed on the curved cylindrical sides (diametrically opposite each other). One of the flat end surfaces of the cylinder is used for flush mounting the test transducer or measuring system under evaluation. The reference transducer is flush mounted on the opposite flat surface. Two additional openings through the cylindrical walls are provided. They can serve independently, in any combination as either inlets or outlets or be plugged. These openings offer additional control of average chamber (bias) pressure independent of the pressure fluctuation amplitude.

Inlet opening area modulation is achieved by rotating a circular disc with equally spaced holes located along a circle near the disc periphery aligned with the inlet nozzle throat. The disc holes are the same size and shape as the nozzle throat. They are spaced one hole diameter apart around the hole-circle. All flow openings are operated at supercritical flow conditions.

The more pertinent operating characteristics of the generator are given in Figures 2 and 3. The oscillation pressure amplitude is a function of frequency. This function is essentially independent of average chamber pressure. Thus the ratio of peak-to-peak pressure amplitude to average chamber pressure may be plotted as a function of frequency and is given in Figure 2. The actual pressure amplitude for any transducer amplitude ratio test point is found by multiplying the ratio by the corresponding chamber pressure. The brackets (pressure amplitude spread) shown on the curve are discussed in the section on test procedure. Figure 3 shows the typical oscillation pressure waveform (filtered and unfiltered) and the corresponding spectral content (frequency and amplitude) of the unfiltered wave at the conditions of 10 kilohertz and an average chamber pressure (static-pressure level) of 150 psia (104 N/ cm^2 abs). The phase difference between the filtered and unfiltered pressure waveforms is due to a 180 degree phase shift by the filter and to the

small difference in oscilloscope external trigger sensitivities on the two oscilloscope time base units used. Waveform is similar at higher frequencies and/or static pressures and somewhat improved (higher harmonics and noise amplitudes are reduced) at lower frequencies and/or static pressures. The frequency spectrum in Figure 3b of the unfiltered pressure waveform shows the relative relationship of the amplitudes of the higher harmonic frequency components as a percent of the amplitude of the waveform fundamental frequency component. The second and third harmonic frequency root-mean-square (RMS) amplitudes are 7 and 5 percent, respectively, of the fundamental frequency RMS amplitude. The corresponding ratio of combined energy in these two harmonic waves to the energy in the fundamental wave associated with the pressure oscillation is less than 0.75 percent.

Transducers

The pressure transducers tested in this program were selected to represent frequently used, current, high-frequency, dynamic pressure transducers. Inquiries were made of most of the National Aeronautics and Space Administration research centers, several Air Force and Navy laboratories, several aerospace companies, several industrial companies, and several pressure transducer manufacturers. The transducers selected were (in alphabetical order):

Kistler Instrument Corporation

Model No. 603A
Model No. 614A/644
Model No. 616

Kulite Semiconductor Products, Inc.

Model No. CQL3-093-15D*

PCB Piezotronics Inc.

Model No. 122M03

Sensotec, Inc.

Model No. SA8J-6H

The selected pressure transducers used in the test program are shown in Figure 4.

* Transducer is essentially flush mounted in a special gas bleed NASA-LeRC holder.

These transducers include several different transduction and construction types, cooled and uncooled types, and several pressure ranges as well as several of the same type, but differing in manufacturer. These differences and their effects are assessed in the Result and Discussion section.

Instrumentation

Instrumentation was set up in conjunction with the pressure generator to measure generator pressure oscillation frequency and pressure amplitude of the transducer under test and of the reference transducer. A schematic diagram of the measuring system layout is shown in Figure 5. Frequencies were measured with an electronic counter and a magnetic pickup which sensed or counted the holes in the generator rotating disc. For pressure amplitude measurements, the conditioned signals were filtered and displayed on a high frequency dual beam oscilloscope. The oscilloscope was externally triggered by a manually operated switch in a trigger line between the IM-SPG and the oscilloscope. Another magnetic pickup provided the trigger signal by sensing a single notch on the outer periphery of the rotating chopping disc. Thus, the same holes and their resultant pressure oscillations were measured in each test providing consistent test conditions. Pressure amplitude of the reference transducer was also measured by a high-frequency true root-mean-square meter and manually recorded. This latter measurement provided a quick check on pressure amplitude. A 50 kilohertz low-pass filter was used to smooth out any small suppressed transducer ringing remaining in the signal (see Figure 3) for data reduction accuracy. A single channel spectrum analyzer (storage oscilloscope plug-in unit) was used to check waveshape consistency above that obtainable from visual observation of the wave form trace on the oscilloscope. In addition to static calibrations, all instruments and the integrated systems were calibrated for frequency response using a high-frequency electronic signal generator. It was found that the output of the charge amplifiers used for conditioning the piezoelectric pressure transducer signals had to be corrected in amplitude at high frequencies and high amplification levels. The low-pass filter and charge amplifier frequency response characteristics are given in the Appendix.

Procedure

Static pressure calibrations were performed on all transducers originally planned for use in this program. However, failure at the start of testing of several Kistler transducers normally used as reference transducers in past transducer test programs resulted in the use of substitution transducers. Two additional Kistler Model No. 603A transducers were obtained. One was used as the reference transducer and the other as a test evaluation transducer. Calibration data supplied by the manufacturer were used for data reduction on these transducers.

All transducers (including the Kulite transducer which had been installed in a special NASA-LeRC housing) were flush mounted into the IM-SPG

test chamber. A 0.007-inch thick flat annular spacer tape was used to keep the transducer sensing surface or passage from contacting the IM-SPG chamber acoustic filler.

Estimated accuracy of the frequency measurement is $\pm$ 1 hertz. The cycle-to-cycle variation in oscillation pressure amplitude on both the reference and test transducer output signals was found to be $\pm$ 2 percent in the worst cases. This is within and includes the inaccuracies due to reading the oscilloscope photographs, electronic noise, and the chamber pressure transducer and gages for chamber pressure measurements used in Figure 2.

The test-to-test variation or repeatability of oscillation pressure amplitude as measured by the reference transducer and of average chamber pressure each time the generator was turned on at any frequency was found to be normally $\pm$ 2 percent, and to reach $\pm$ 5 percent in a few cases. These percentages were obtained when the test transducer mounting plug remained fixed (not removed and reinserted or changed) in the generator chamber. They also include the variation or scatter of the inlet pressure to the generator which controls the average chamber pressure and is of the same order-of-magnitude.

During the calibration of the test transducers the test transducer mounting plug was changed intermittently throughout the test series. All test transducers to be tested at a particular average chamber pressure and series of frequencies were tested at that pressure condition. Thus the test transducer mounting plug was repeatedly changed at that pressure level. The test-to-test variation in oscillation pressure amplitude in the IM-SPG as measured by the reference transducer was found to be much greater during the testing of the transducers involving the changing of the test transducer mounting plugs and was much greater than the $\pm$ 2 to $\pm$ 5 percent variation for a fixed plug. This changing in oscillation pressure amplitude was random with each mounting plug change. The amount of spread and the relative value within the scatter of the oscillation pressure amplitudes between transducer tests changed at each average chamber pressure. These variations are possibly due to minute movements of the acoustic absorbing filler at each changing of the transducer mounting plug.

Normally such changes in oscillation pressure amplitude would be of small consequence in comparative calibrations because the test transducer response is being compared to the known reference transducer response and it are known that the oscillation pressure amplitude and average chamber pressure is identical at each transducer location. This has been verified in the IM-SPG with an empty chamber. It was not determined in the present program if both sides of the generator chamber (across the filler) at each transducer location had these requirements of corresponding oscillation pressure amplitude and average chamber pressure. Consequently, the spread in oscillation pressure amplitude measured by the reference transducer at each average chamber pressure and frequency has been assumed as possibly existing between test and reference transducers and was used to establish error band brackets for the test transducer amplitude ratio data. This is believed to be a rather severe, but bounding assumption.

The error bands were determined by a weighting process by using the total spread of oscillation pressure amplitude measured by the reference transducer of all of the test transducers calibrated at a set frequency and average chamber pressure. First the arithmetic average of all reference transducer oscillation pressure amplitudes at the set conditions was made. Then the ratio of the largest amplitudes above and below the mean to the mean was calculated. Then the ratio of the reference transducers amplitude associated with a particular test transducer to the mean was determined. The plotted data point for that transducer and its associated upper and lower error band limits was then determined by multiplying the above three ratios by that test transducers dynamic response ratio at the set calibration condition. This procedure was performed for each test transducer at each calibration condition. Thus in the data plots the position of a data point in its error band indicates where the reference transducers measured oscillation pressure amplitude was for that test transducer relative to the spread of amplitudes for all test transducers at each average pressure and frequency. The dynamic response ratio as a function of average chamber pressure for one frequency was determined in a similar manner.

IM-SPG is capable of operating with any gas. Hydrogen, helium, and nitrogen are normally used. For this test program hydrogen was used for all tests. Lower cost, greater dynamic amplitude, and higher frequency range are achieved using hydrogen.

RESULTS AND DISCUSSION

The dynamic response characteristics of the test transducers are given in the form of amplitude ratio and plotted in Figures 6-20. The amplitude ratio is given for all transducers except the low-pressure Kulite transducer as a function of frequency at one static-pressure level and as a function of static-pressure level at one frequency, 3 kilohertz. For the low-pressure Kulite transducer only amplitude ratio as a function of frequency was performed. Two amplitude ratios are generally given for each of the conditions. The first is the normally used amplitude ratio, the ratio of the test transducer oscillating pressure signal to the reference transducer oscillating pressure signal. It is represented in each figure by a solid line. The second amplitude ratio is the ratio of the test transducer oscillating pressure signal to the oscillating pressure signal of the Kistler Model No. 603A on the test side of the SPG chamber. It is thus a ratio to the same side of the chamber and is an attempt to minimize or eliminate possible side-to-side IM-SPG oscillating pressure amplitude differences. This latter ratio is indicated by a dashed line in each figure.

The 603A test transducer was not tested at the pressure-frequency combinations of the lower pressure Sensotec and Kulite transducers. For the amplitude ratio of these low-pressure test transducers to the 603A test transducer, the 603A test transducer results were extrapolated. For the Sensotec transducer, the lower bias pressures of the 603A were extrapolated linearly

with frequency using the test 603A frequency response at 150 psia (104 N/(cm)^2 abs). For the Kulite transducer, the 603A bias pressure curve at the three kHz was extended to 15 psia (10.4 N/(cm)^2 abs) and same linear variation with frequency of the 603A at 150 psia (104 N/(cm)^2 abs) was applied. These extrapolations are shown on Figure 14.

In general none of the transducers gave the same measurement of the sinusoidal pressure amplitude as the reference transducer (i.e., amplitude ratio of 1.0). This is also true for pressure signals referenced to the test transducer side of the chamber. This is true even when consideration is given for assumed differences in oscillatory static pressure across the chamber, which is represented by the error band brackets in Figures 6-18. The principal conclusion drawn from Figures 6-20 is therefore that dynamic pressure measurements given by the various transducers differ from one another and should be accounted for.

The characteristics of the test data are discussed in the following two sections, Effects of Frequency and Effects of Static Pressure, without consideration of differences in the transducers. The effects of transducer differences such as transduction type, protective passages and bleed flow, etc., are discussed in the section, Other Effects.

Effects of Frequency

All of the transducer plots of amplitude ratio as a function of frequency (Figures 6-12) were ragged in appearance. Few were constant over the entire frequency range on a frequency point-to-point basis. Some of this can of course be considered to be caused by the possible pressure amplitude difference conditions. However, a principal conclusion that can be drawn is that the response of all of the transducers is flat (in a relative sense) to within $\pm$ 10 percent about the individual test transducers average value of amplitude ratio up to frequencies of 10 kilohertz and are flat to within $\pm$ 15 percent about the average value up to frequencies of 15 kilohertz, except for the Kistler Models 614A and 616 at 15 kilohertz.

All of the transducer amplitude ratios of each type are plotted in Figure 13 to show relative comparisons (without error bands for clarity). The major characteristics seen are:

(1) The relative flatness of the transducers up to 10 kHz

(2) The divergence after 10 kHz

(3) The differences in dynamic transducer sensitivities.

These characteristics are discussed in the following two sections, Effects of Static Pressure and Other Effects.

Effects of Static Pressure

The amplitude ratios of the test transducers as a function of static pressure are shown in Figures 13-18 and 20. All of the tests were performed at one frequency, 3 kilohertz. No pressure level variation tests were performed for the low pressure range (15 psid) (10N/ cm ^{2} d) Kulite transducer. The lack of a significant pressure difference and the large sinusoidal pressure fluctuations at low frequency precluded this.

The amplitude ratios are again seen to be jagged and nonlinear. The responses of all of the transducers were affected by static pressure level. The most general conclusion that can be drawn from this test series is that this effect was larger than the frequency effect over the frequency range covered. From there any trends are less clear due to generally somewhat opposing results of the two amplitude ratio plots. With the exception of the Sensotec transducer, all of the other transducers showed a general decreasing amplitude ratio toward a unity ratio at 300 psia (204N/ cm ^{2}abs) with increasing pressure based on the amplitude ratio referenced to the reference transducer. The Sensotec showed increasing amplitude ratio with increasing pressure for both types of amplitude ratios. However, based on the amplitude ratio referenced to the test 603A transducer these other transducers showed a slight general trend of increasing amplitude ratio toward a unity ratio at 300 psia (204N/ cm ^{2}abs) with increasing static pressure level and with wider variations about their averages. No explanation could be found for this difference.

The Sensotec and Kulite (at 3 kHz) transducers had the lowest amplitude ratios (Figure 20). Figure 19 shows that these two transducers amplitude ratios were the lowest throughout the frequency range investigated. The Kulite dat at 8 kHz and 15 psia (10N/ cm ^{2}abs) is given with the Sensotec data in Figure 18 and is consistent with the decreasing sensitivities of these transducers with decreasing static pressure.

Other Effects

Tests were performed on the same Kistler Model No. 603A having a uniform 0.025-inch (0.064 N/ cm ^{2}abs) thick Silastic brand RTV coating on the diaphram. The largest effect of the coating that can be inferred from Figures 6, 7 and 13 is that the above average response of the uncoated transducer at 10 kilohertz and the below average response at 15 kilohertz has been shifted down in frequency by 5 kilohertz. However, the average response ratio is still flat to within less than $\pm$ 10 percent when referenced to either the reference transducer or the test transducer. No significant difference due to the coating was observed for the amplitude ratio as functions of bias pressure (Figures 14, 15 and 20).

Three of the transducers, Kistler Model No. 614A/644, Kistler Model No. 616, and PCB Model No. 122M03 had protective passages and associated cavities in front of the transducer sensing surface. The 614A/644 passage is

0.063-inches (0.160 cm) in diameter by 0.187-inches (0.475 cm) long with a 0.003-inch (0.008 cm) long clearance in front of the 0.25-inch (0.64 cm) diameter transducer front surface. The 616 has a passage of 0.067-inches (0.177 cm) in diameter by 0.097-inches (0.247 cm) long with a 0.003-inch (0.008 cm) long clearance in front of the 0.22-inch (0.555 cm) diameter transducer front surface. The 122M03 passage is 0.60-inches (1.53 cm) in diameter by 0.16-inches (0.407 cm) long with a 120 degree cone tapering to 0.1-inch (0.254 cm) in diameter with a 0.003-inch (0.008 cm) long clearance in front of the 0.25-inch (0.64 cm) diameter transducer front surface.

The first effect noted (Figure 13) is that the three transducers listed above had flat dynamic response (within $\pm$ 10 percent) up to 10 kilohertz, but had increased output at 15 kilohertz. A second effect noted is that the transducer with a longer passage (Kistler 614/644) had a dynamic response that was also larger than the transducer with the shorter passages (616 and 122M03). It is interesting to note that the same basic transducer type is used in the three Kistler Models, 603A, 614A/644, and 616. Thus, their amplitude ratios are similarly flat to 10 kilohertz and have increasing response at 15 kilohertz consistent with the addition of increasing protective passage length.

The effects of cooling gas (bleed) on transducer response were investigated on the two transducers employing the bleed gas technique, Kistler Model No. 614/644 and Kulite Model CQ3-093-15D in the NASA-LRC housing. Generally, helium is employed as the bleed gas. Hydrogen, which was used as the IM-SPG test gas for all tests, was also used as the bleed gas in these measurements. For the coolant effects studies, additional tests were performed on these two transducers using nitrogen and also with no-bleed or coolant flow. Tests on the Kistler were performed at 3 kHz (Figure 16) and on the Kulite at 3 and 10 kHz (Figure 12). The helium bleed performance should be bounded by that of the hydrogen and nitrogen. In general, there were changes in amplitude ratio for the nitrogen and no-bleed cases as compared to using hydrogen bleed gas. No trend was established however.

The only conclusion that can be made with regard to transduction type is that the piezoelectric types had higher dynamic sensitivities than the two strain gage types (bonded strain gage Sensotec, diffused strain gage Kulite). See Figures 13 and 20. This may be caused by sensing area differences, diaphragm material differences (metal versus silicon), or by the bleed in front of the Kulite. The two strain gage types had a flatter dynamic response up to 10 kilohertz.

SUMMARY OF RESULTS

The pressure transducers tested, under the limitations of the possible oscillating static pressure amplitude difference across the pressure generator chamber, showed the following results:

1. All of the transducers exhibited frequency dependent response although most were flat (± 10%) to 10 kilohertz.

2. All of the transducers exhibited a dynamic response which depended on static pressure level. The general trend (increasing or decreasing response) was not clearly established, but its effect was always larger than frequency dependent effects.

3. The various transducers had different dynamic pressure outputs (sensitivities) than those based on static calibrations. It was not possible in this investigation to establish the absolute dynamic calibration for any given transducer tested.

CONCLUDING REMARKS

The differences indicated in dynamic sensitivity as compared to static sensitivity and its dependency on static pressure between the various transducer types appears to be over and above the uncertainty scatter in the results. The comparatively large effects, greater than ± 10 percent for each effect (Figure 20), indicate that these questions should be resolved. Further work is necessary to pinpoint the magnitude of these effects.

APPENDIX

CORRECTIONS TO DATA

The reference and test pressure transducers output signals were each conditioned by a charge amplifier and then filtered. The charge amplifiers were used at all times for consistency although they were required only for the low-level outputs at the lower pressures. The charge amplifiers were calibrated for dynamic response in accordance with the manufacturers instructions. The transducer data were corrected using the dynamic response characteristics so determined and given in Figures A-1a and A-1b. Similar calibration and corrections were performed for the high-frequency dual-channel filter. These data are given in Figure A-1c.

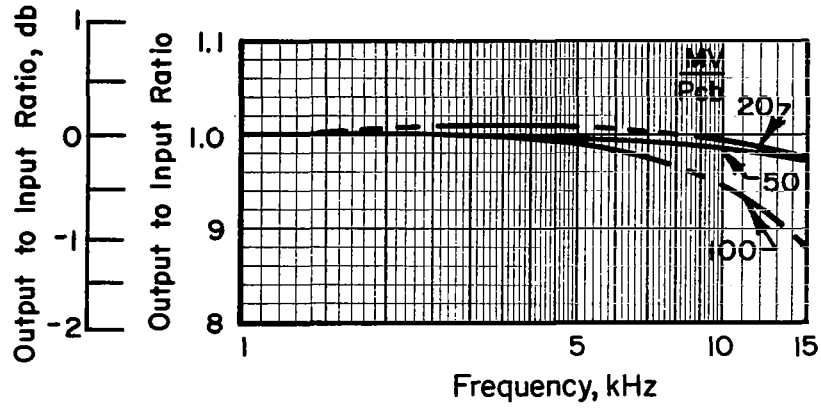

a. Reference Transducer Charge Amplifier

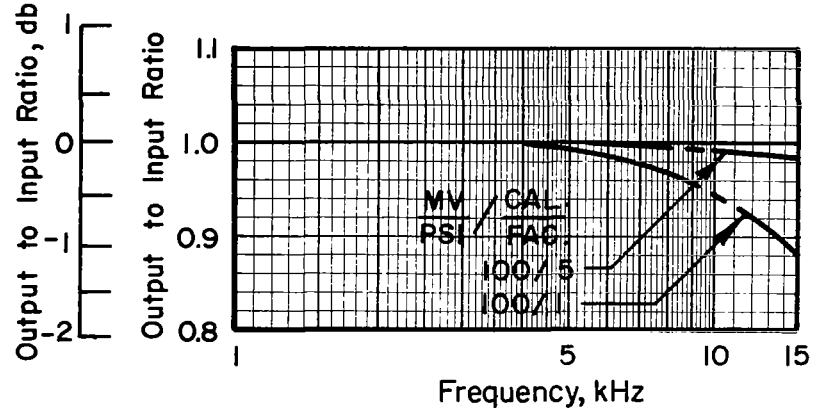

b. Test Transducer Charge Amplifier

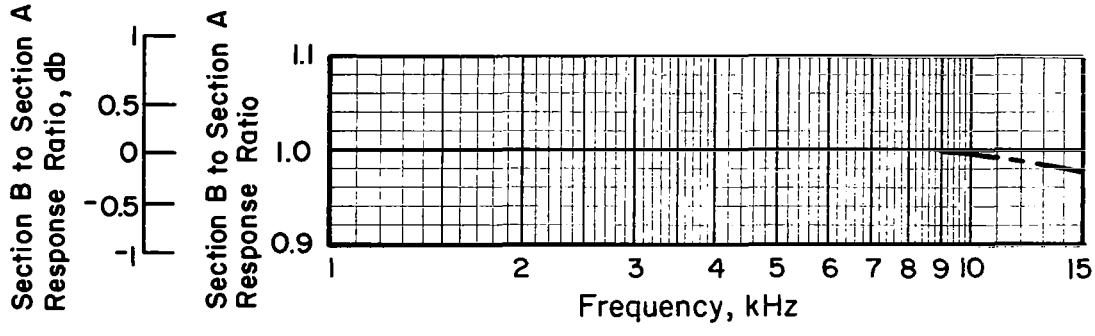

c. Dual Channel Filter

FIGURE A-I. SIGNAL CONDITIONING EQUIPMENT FREQUENCY RESPONSE CHARACTERISTICS.

REFERENCES

(1) Robinson, R. E., and Liu, C. Y., "Resonant Systems for Dynamic Transducer Evaluations", NASA CR-72435 (August 31, 1968).

(2) Robinson, R. E., "Development of a Sinusoidal Pressure Generator for Pressure Transduce Dynamic Calibration", NASA CR-72656 (March 25, 1970).

(3) Robinson, R. E., "Improvement of a Large-Amplitude Sinusoidal Pressure Generator for Dynamic Calibration of Pressure Transducers," NASA CR-120874 (February 1972).

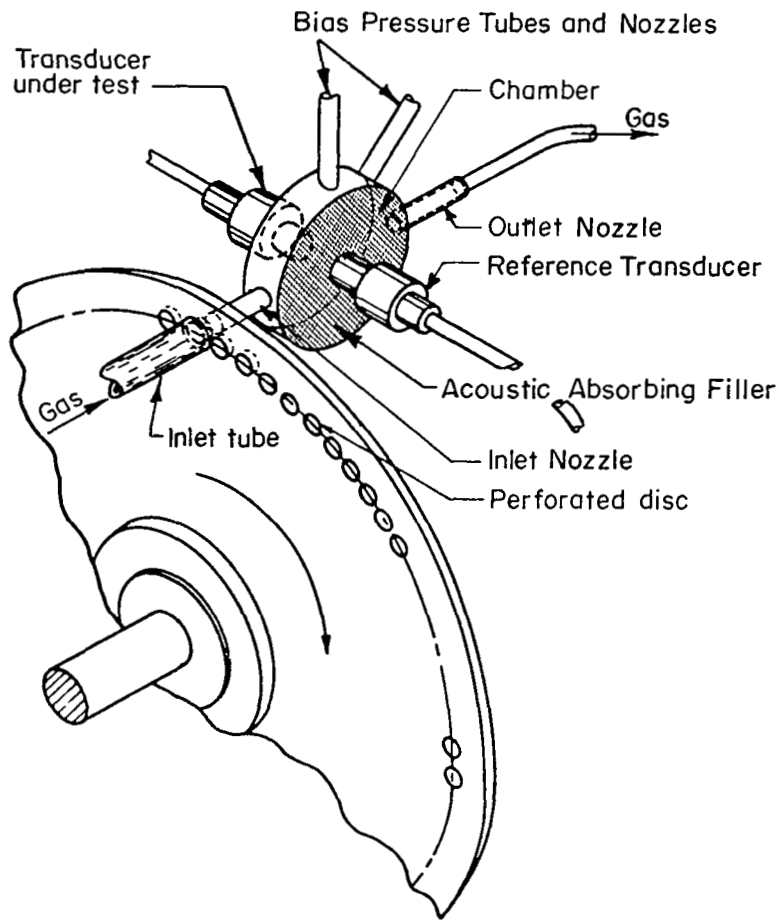

FIGURE I. INLET-MODULATED SINUSOIDAL PRESSURE GENERATOR

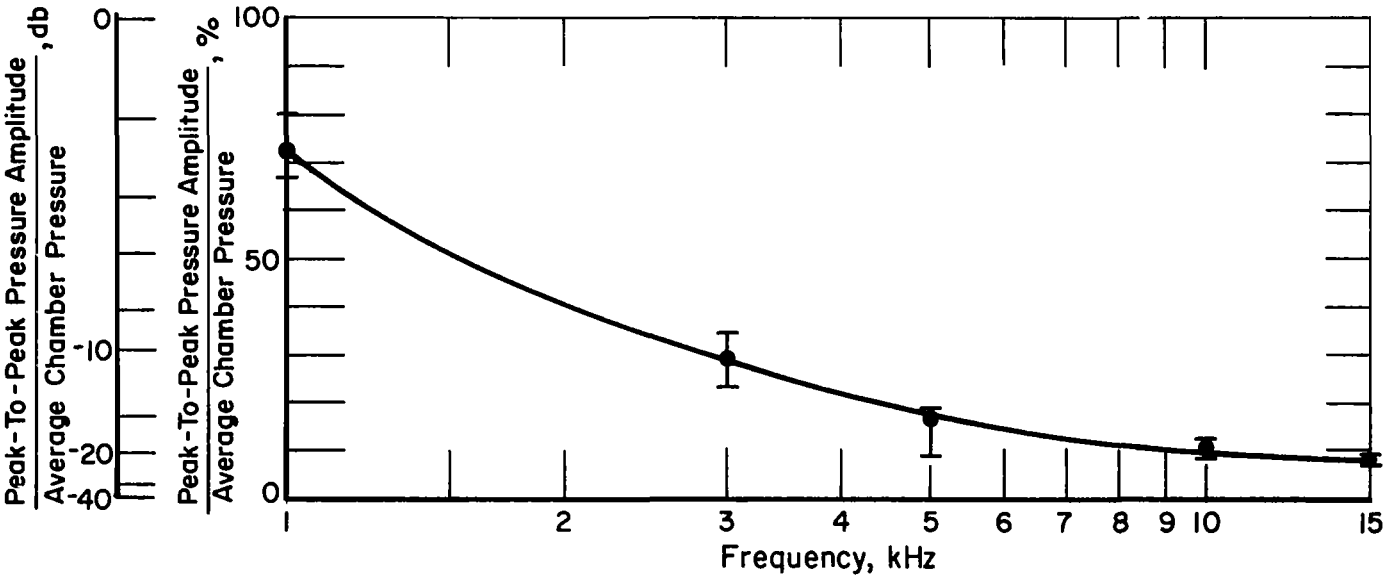

FIGURE 2. SINUSOIDAL PRESSURE GENERATOR EVALUATION TEST CONDITIONS USING HYDROGEN AS THE TEST GAS

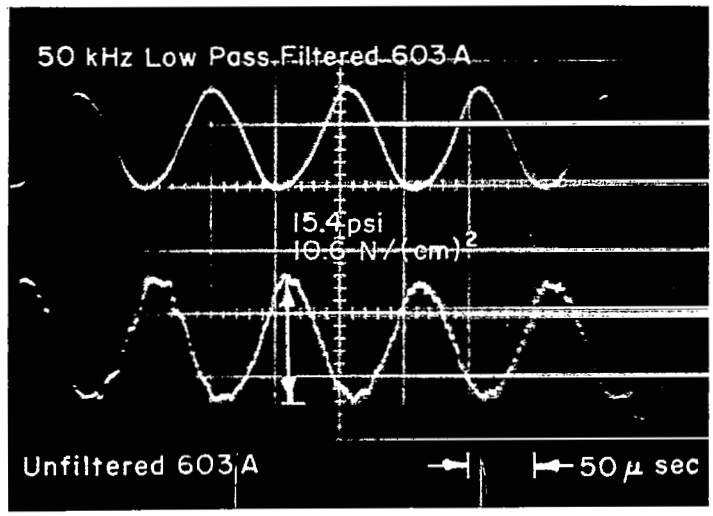

a. Wave Shape

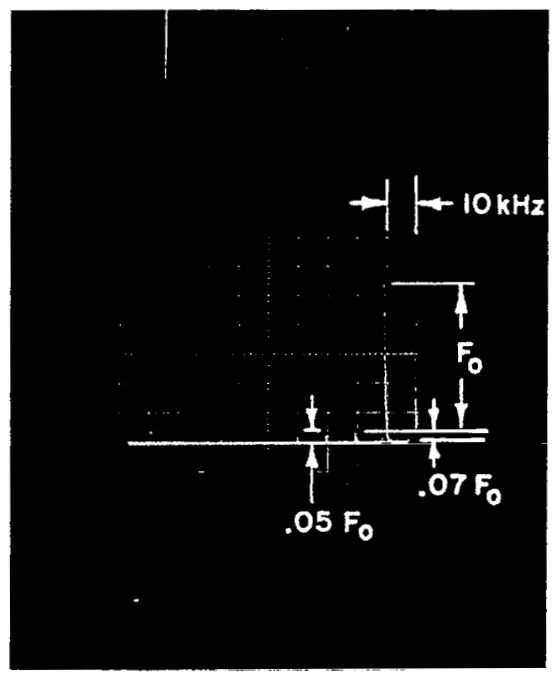

b. Frequency Spectrum

FIGURE 3. PRESSURE WAVE SHAPE AND FREQUENCY SPECTRUM FROM OSCILLOSCOPE. FREQUENCY, 10 kHz; STATIC PRESSURE LEVEL, 150 psia (104 $\frac{N}{cm^2}$) abs; REFERENCE TRANSDUCER

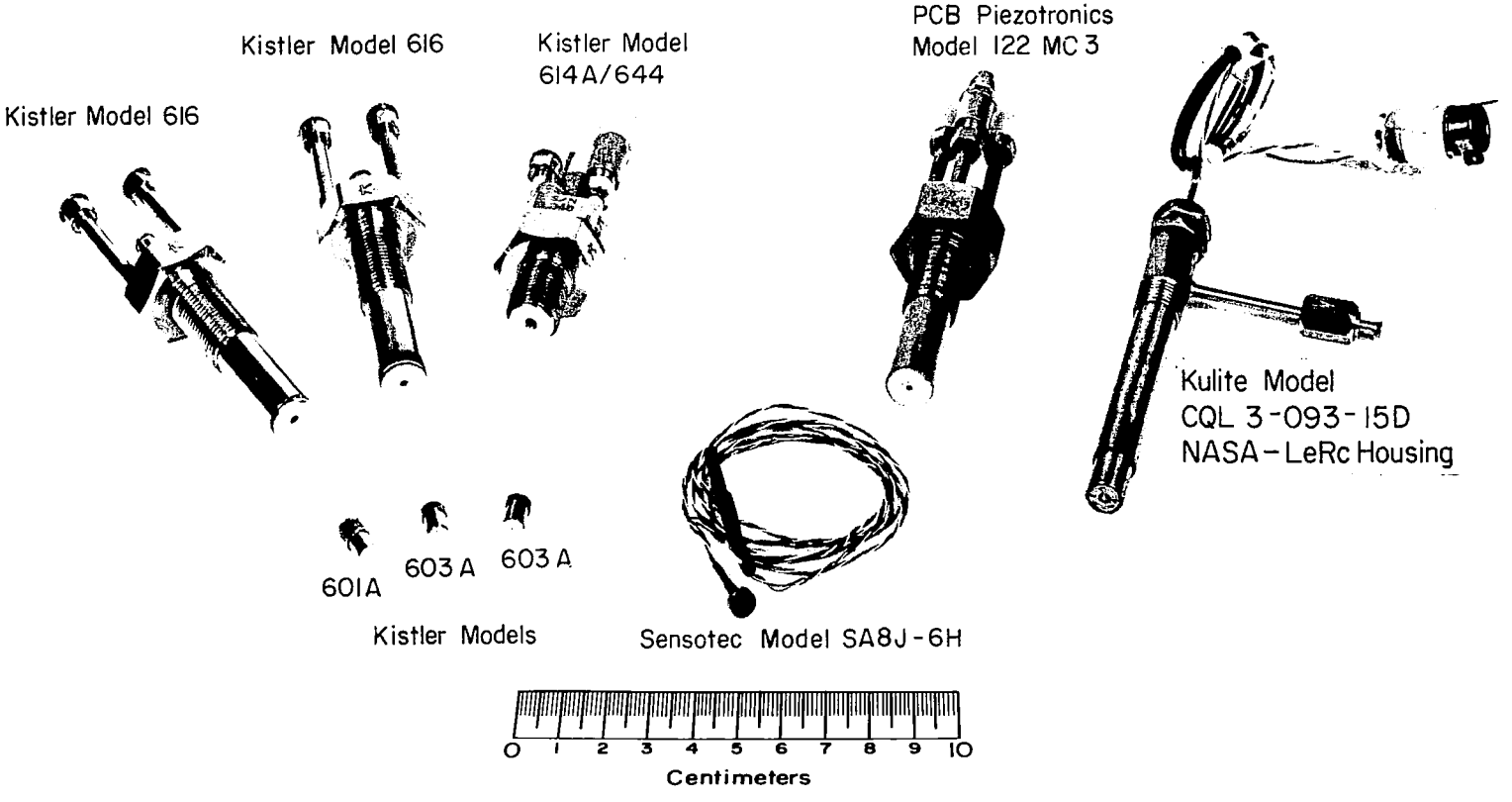

FIGURE 4. PRESSURE TRANSDUCERS USED IN TEST PROGRAM

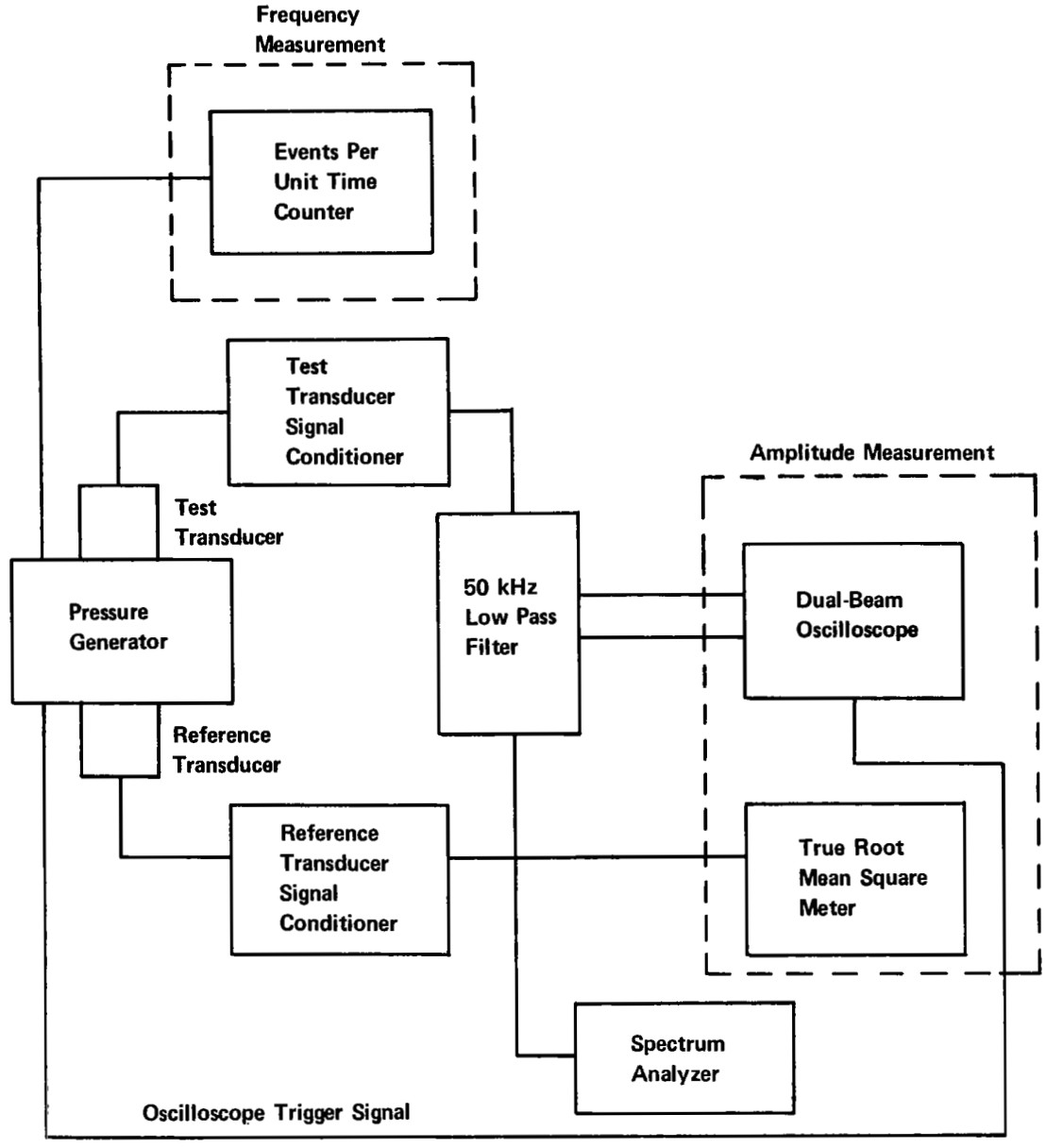

FIGURE 5. TEST APPARATUS LAYOUT

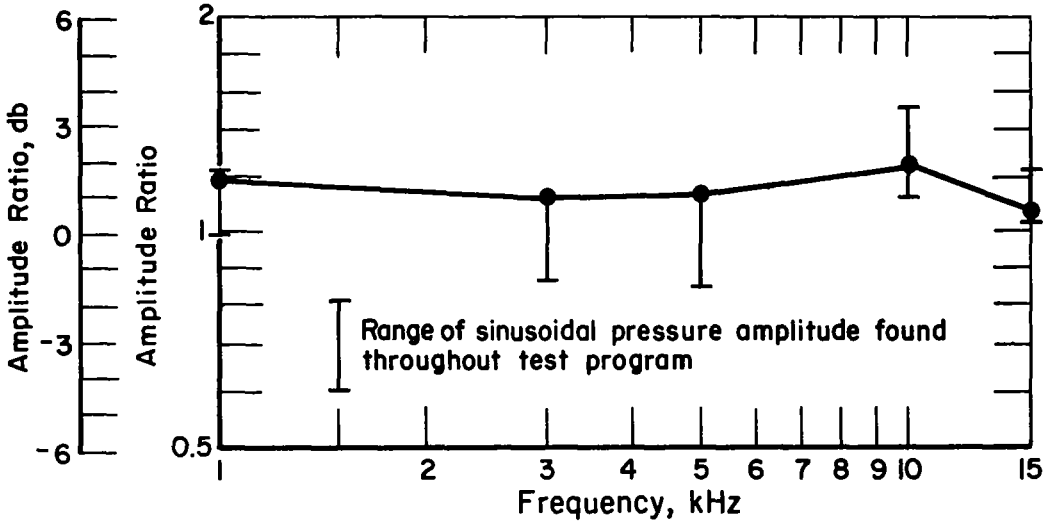

FIGURE 6. AMPLITUDE RATIO VS FREQUENCY FOR KISTLER MODEL 603A SERIAL NO. 2275. STATIC-PRESSURE LEVEL, 150 psia $\left(104 \frac{N}{cm^2} \text{ abs}\right)$

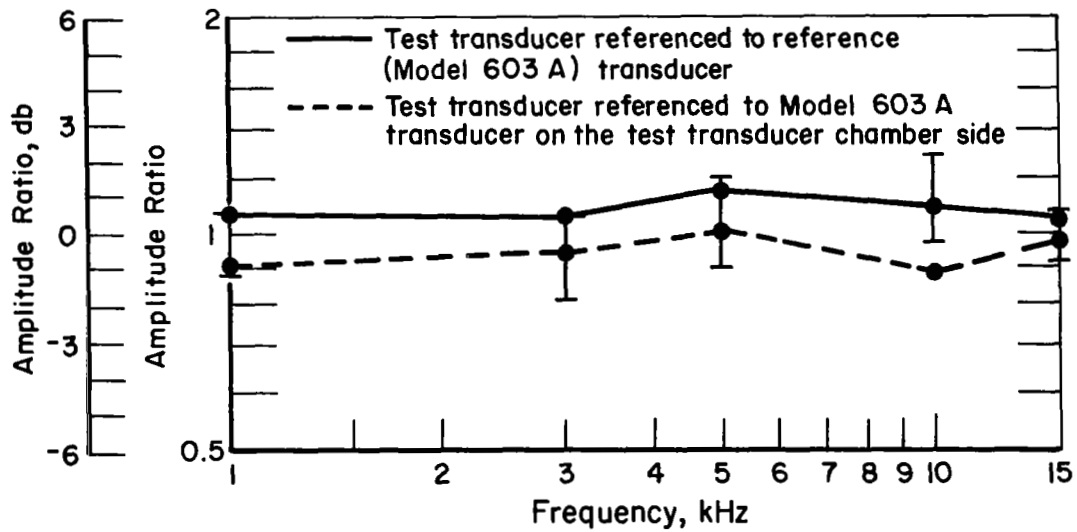

FIGURE 7. AMPLITUDE RATIO VS FREQUENCY FOR KISTLER MODEL 603A, SERIAL NO. 2275. 0.025-in (0.064 cm) SILASTIC COATING ON DIAPHRAM; STATIC-PRESSURE LEVEL, 150 psia $\left(104 \frac{N}{cm^2} \text{ abs}\right)$

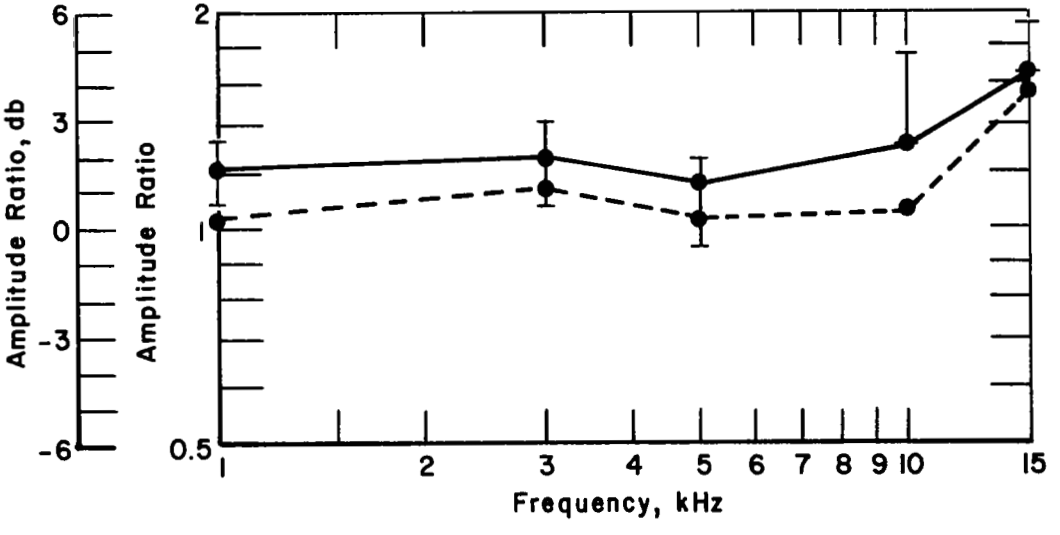

FIGURE 8. AMPLITUDE RATIO VS FREQUENCY FOR KISTLER MODEL 614A, SERIAL NO. 348; STATIC-PRESSURE LEVEL, 150 psia $\left(104 \frac{N}{cm^2} \text{ abs}\right)$

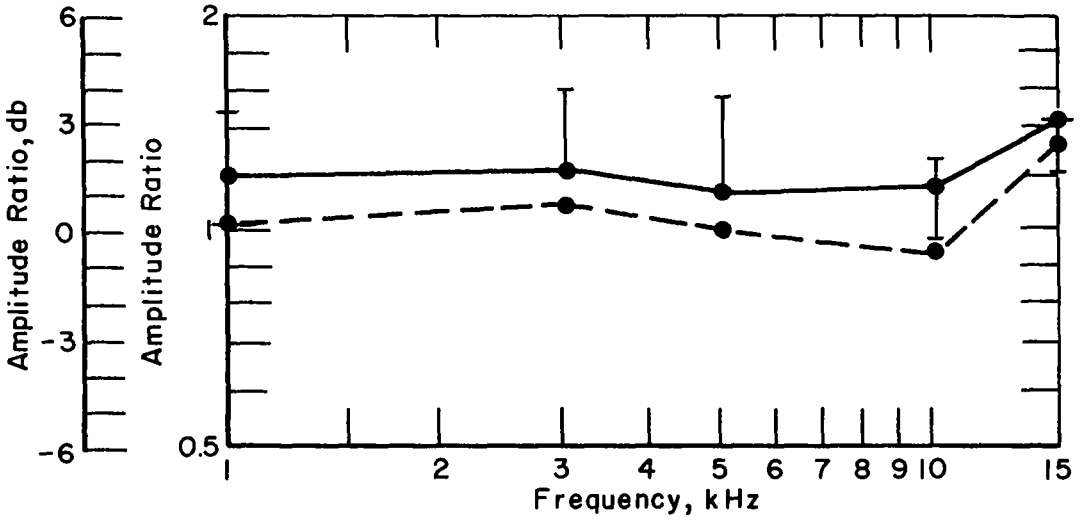

FIGURE 9. AMPLITUDE RATIO VS FREQUENCY FOR KISTLER MODEL 616 SERIAL NO. 1692 STATIC-PRESSURE LEVEL, 150 psia $\left(104 \frac{N}{cm^2} \text{ abs}\right)$

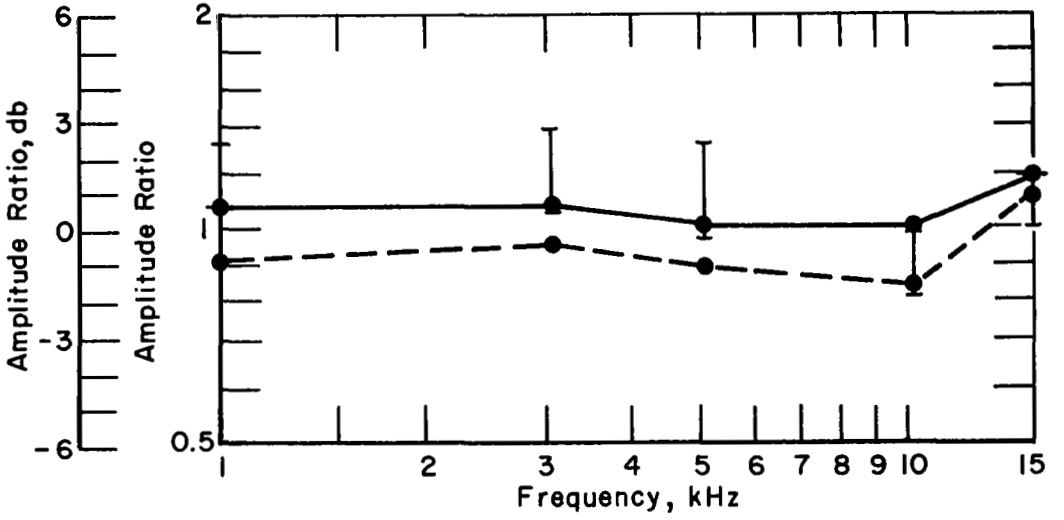

FIGURE 10. AMPLITUDE RATIO VS FREQUENCY FOR PCB MODEL 122 M03 SERIAL NO. 108. STATIC-PRESSURE LEVEL, 150 psia ($104 \frac{N}{cm^2}$ abs)

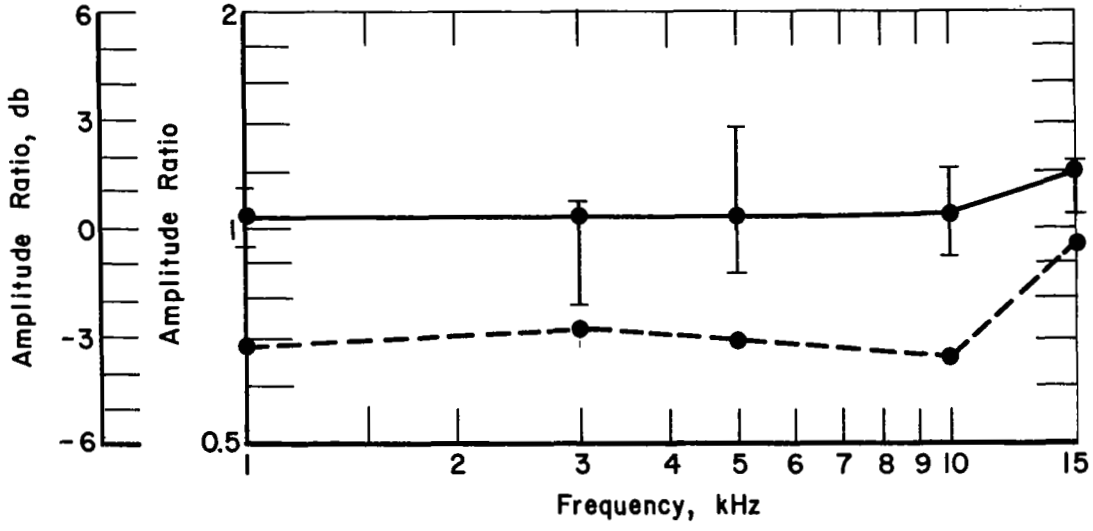

FIGURE 11. AMPLITUDE RATIO VS FREQUENCY FOR SENSOTEC MODEL SA8J-6H, SERIAL NO. 5563; STATIC-PRESSURE LEVEL 45 psia $\left(31 \frac{N}{cm^2} \text{ abs}\right)$

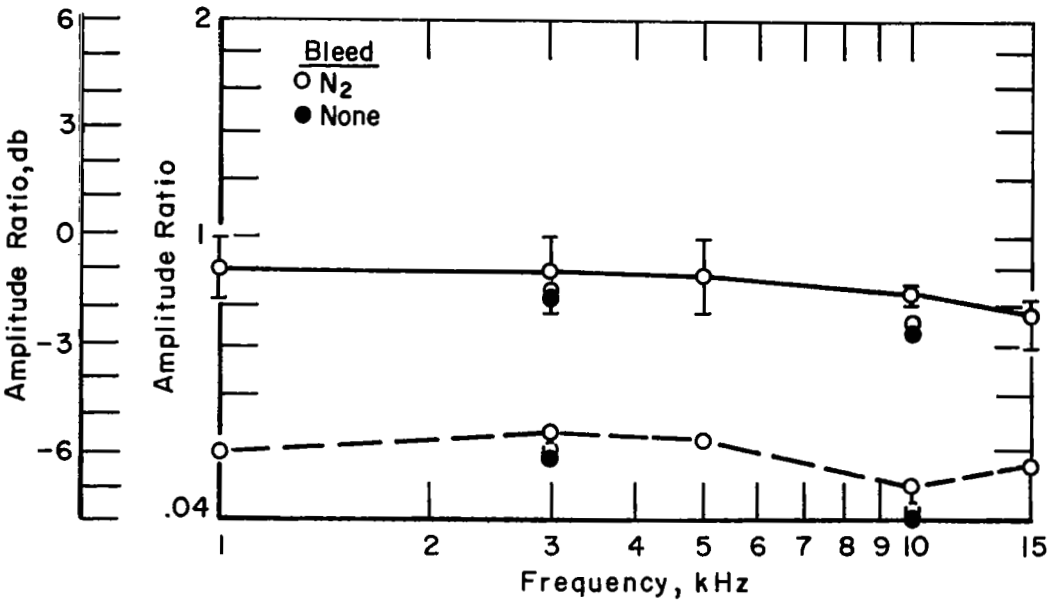

FIGURE 12. AMPLITUDE RATIO VS FREQUENCY FOR KULITE MODEL CQL3-093-15d, SERIAL NO. 1808-4-48; STATIC-PRESSURE LEVAL, 15 psia ($10 \frac{N}{cm^2}$ abs)

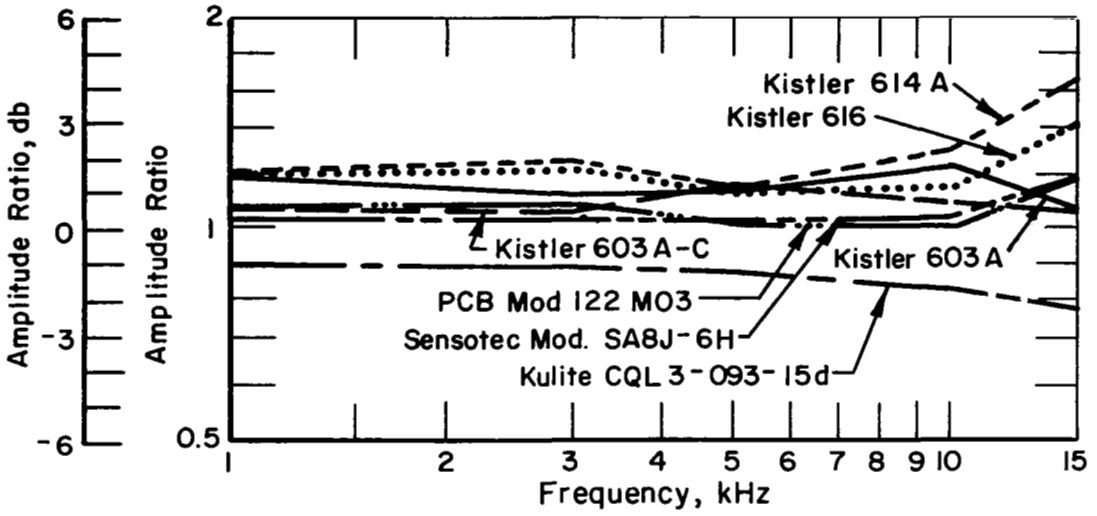

a. Amplitude Ratio vs Frequency, Referenced to Reference Transducer

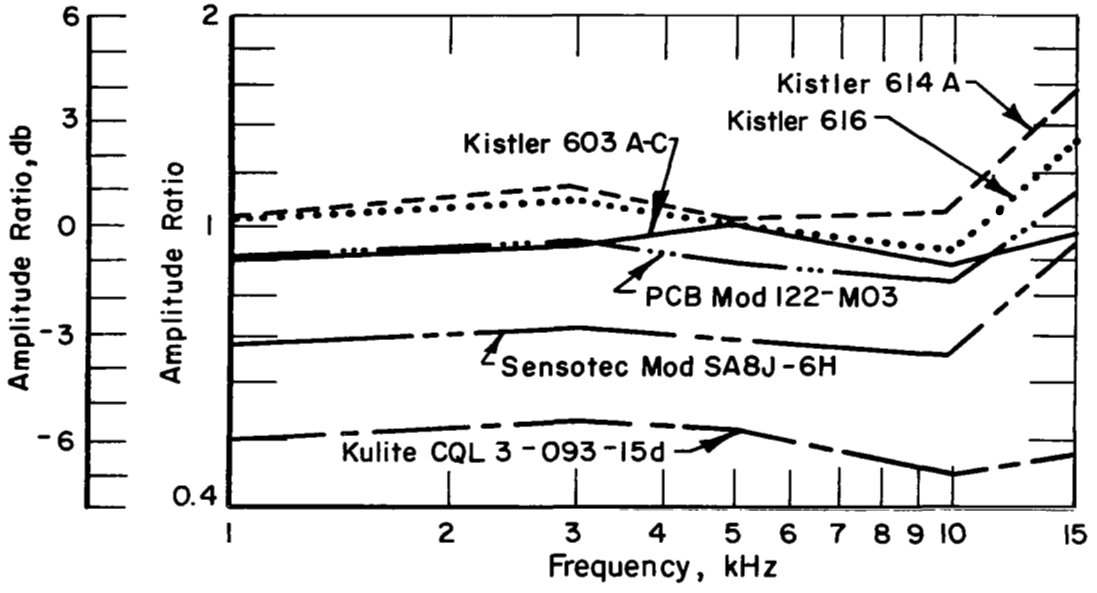

b. Amplitude Ratio vs Frequency, Referenced to Test Kistler 603 A

FIGURE 13. AMPLITUDE RATIO vs FREQUENCY FOR ALL TRANSDUCERS

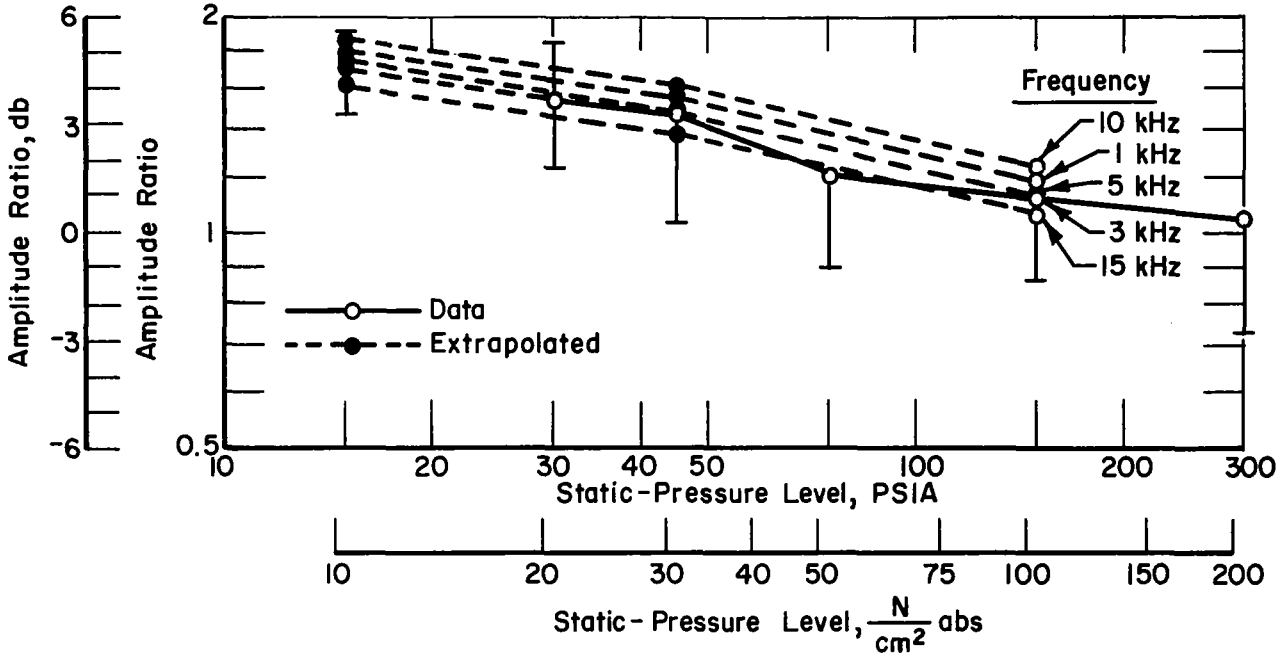

FIGURE 14. AMPLITUDE RATIO VS STATIC-PRESSURE LEVEL AT VARIOUS FREQUENCIES FOR KISTLER MODEL 603A SERIAL NO. 2275. INCLUDES EXTRAPOLATED CONDITIONS USED TO RATIO TEST TRANSDUCER TO TEST TRANSDUCER SIDE OF SINUSOIDAL PRESSURE GENERATOR

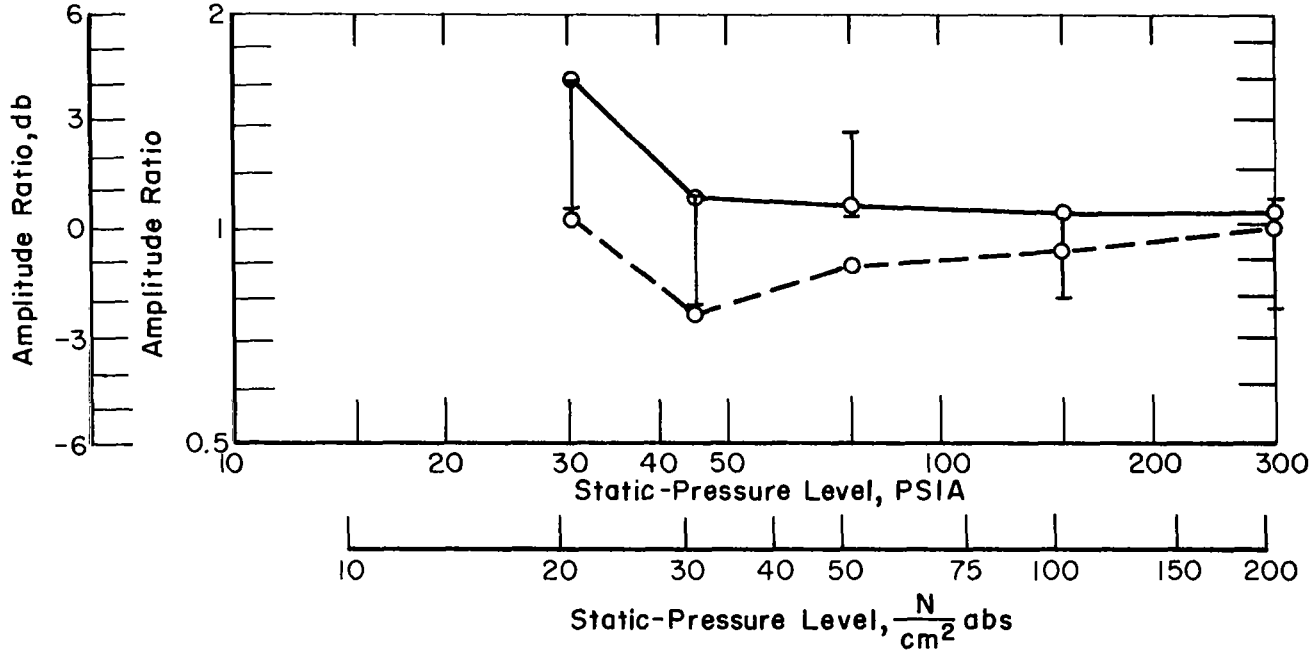

FIGURE 15. AMPLITUDE RATIO VS STATIC-PRESSURE LEVEL FOR KISTLER MODEL 603 A SERIAL NO. 2275 SILASTIC DIAPHRAM, 0.025 INCH (0.064 cm); FREQUENCY, 3 kHz

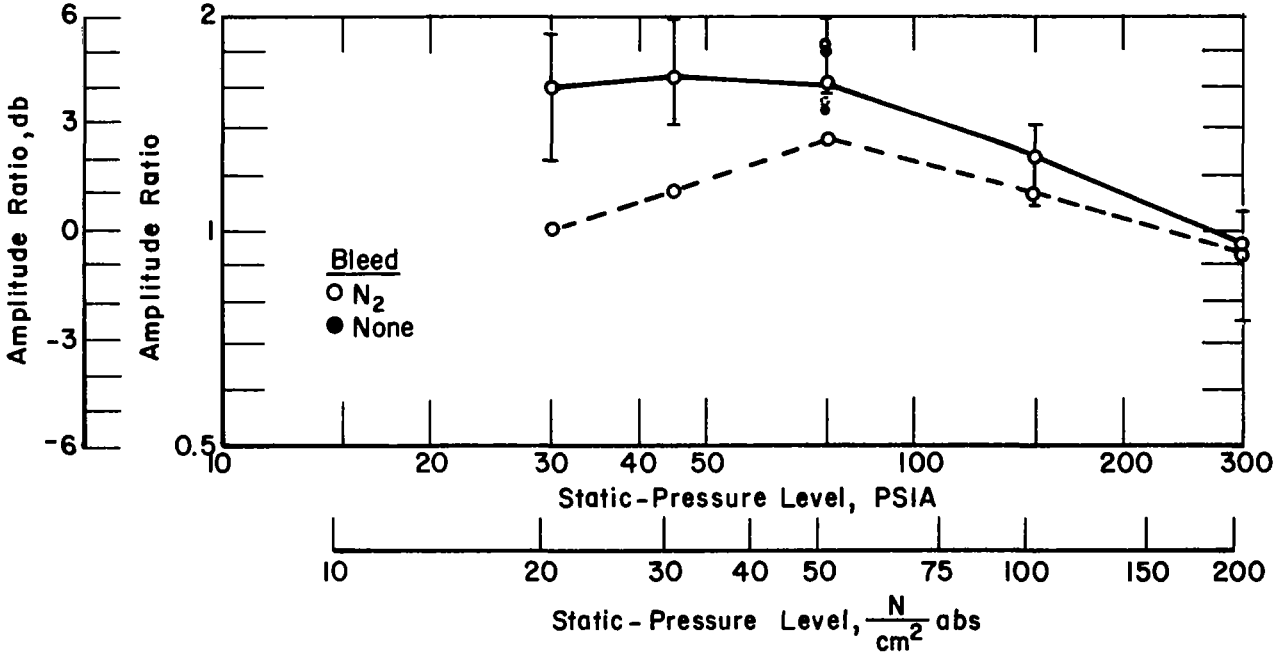

FIGURE 16. AMPLITUDE RATIO VS STATIC-PRESSURE LEVEL FOR KISTLER MODEL 614A/644 SERIAL NO. 348; FREQUENCY, 3 kHz

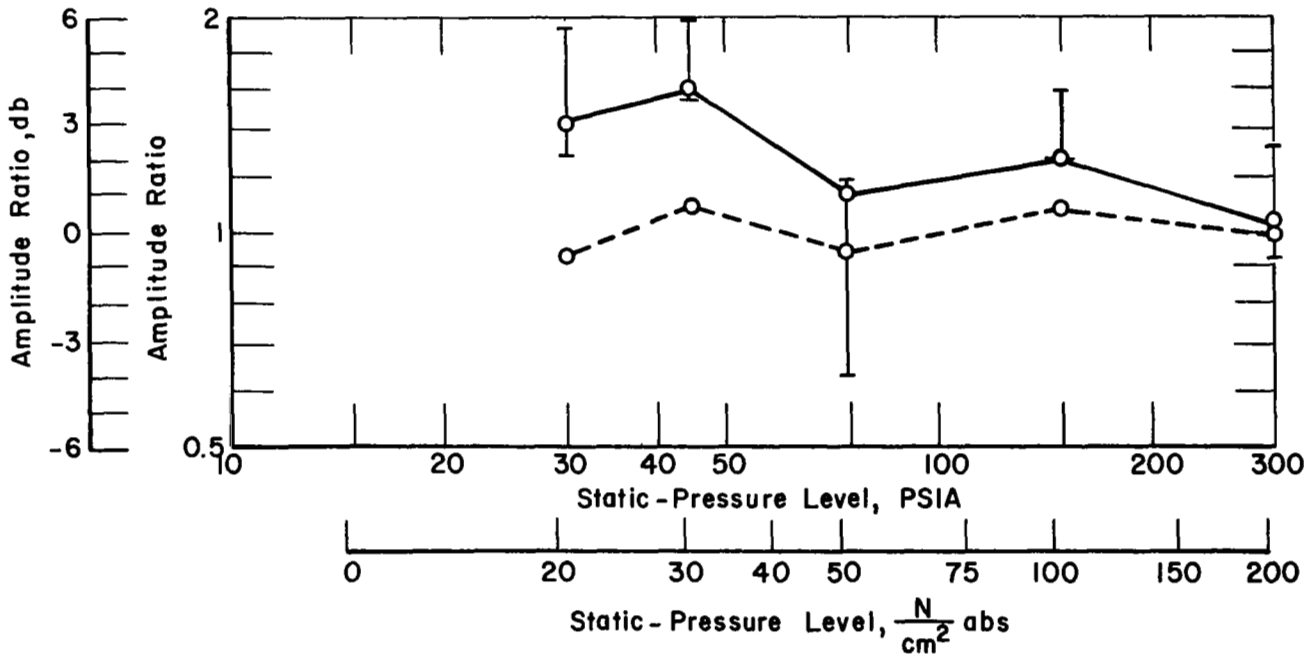

FIGURE 17. AMPLITUDE RATIO VS STATIC-PRESSURE LEVEL FOR KISTLER MODEL 616 SERIAL NO. 1692; FREQUENCY, 3 kHz

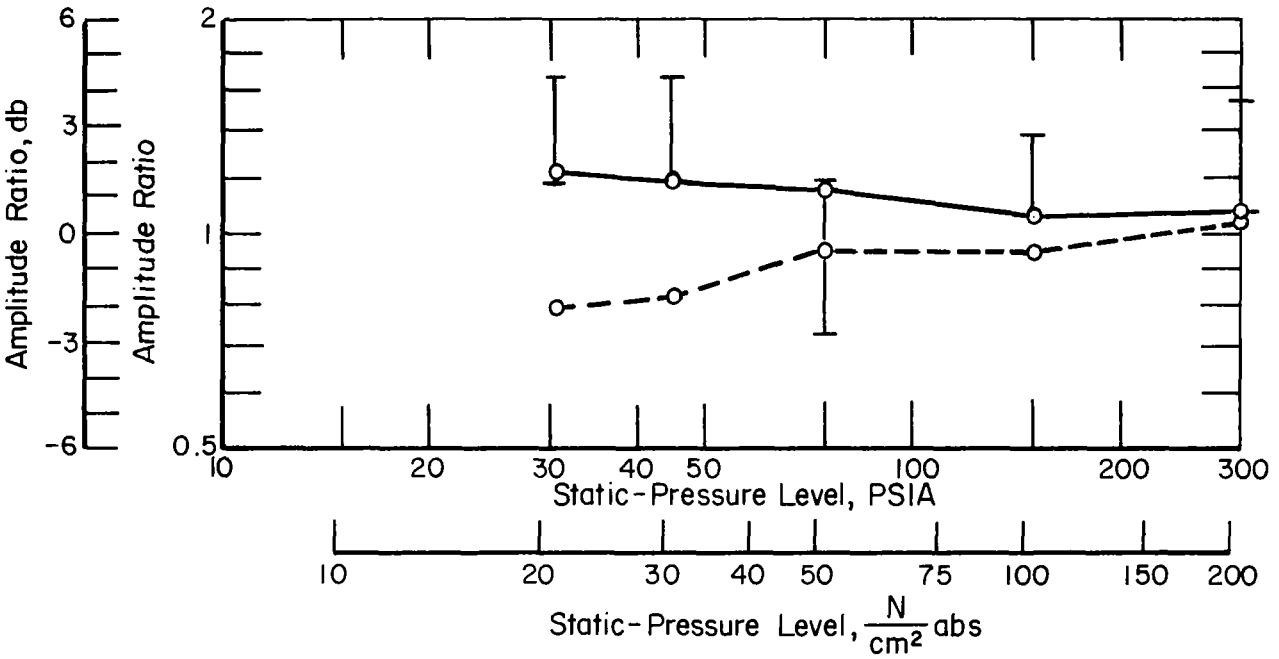

FIGURE 18. AMPLITUDE RATIO VS STATIC-PRESSURE LEVEL FOR PcB MODEL 122 M03 SERIAL NO. 108. FREQUENCY, 3 k Hz

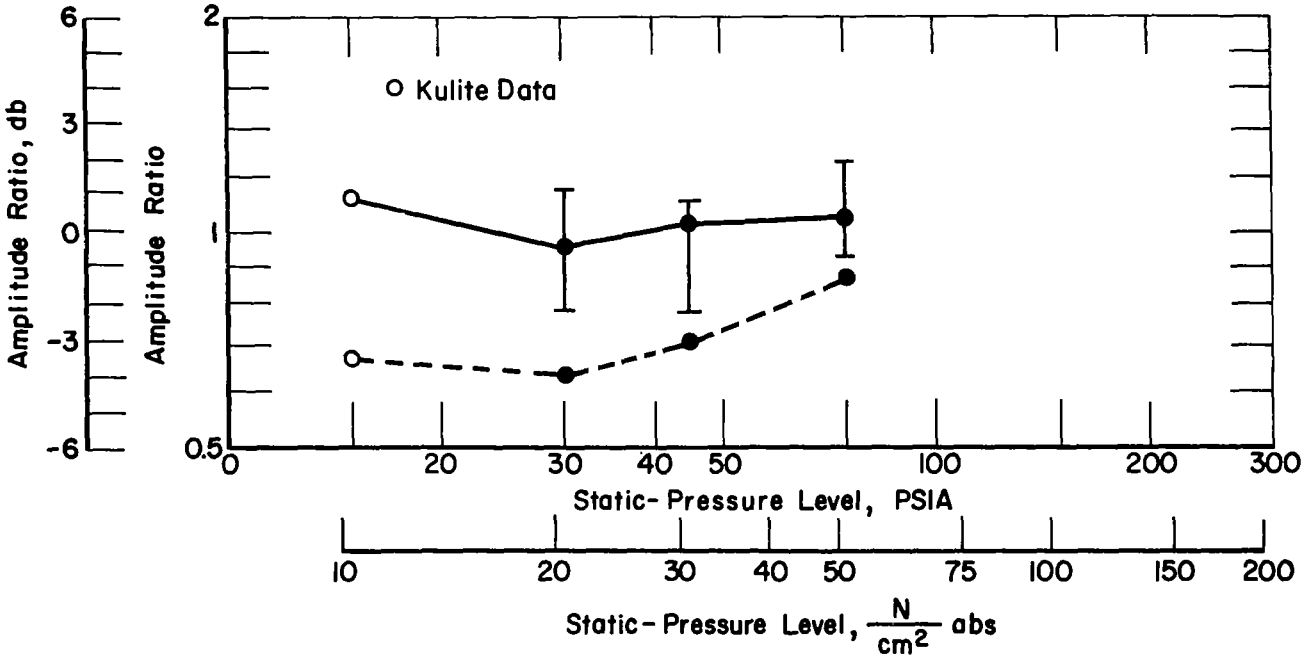

FIGURE 19. AMPLITUDE RATIO VS. STATIC-PRESSURE LEVEL FOR SENSOTEC MODEL SA8J-6H, SERIAL NO. 5563 AND KULITE MODEL CQL3-093-15d; FREQUENCY, 3 kHz

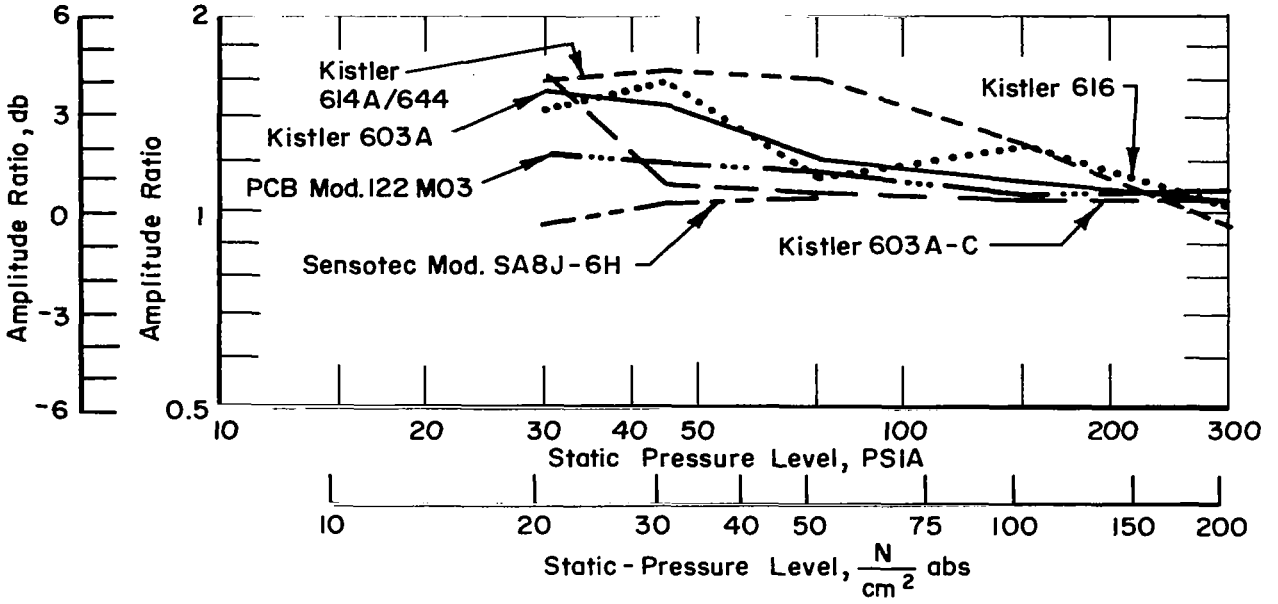

a. Amplitude Ratio vs Frequency, Referenced to Reference Transducer

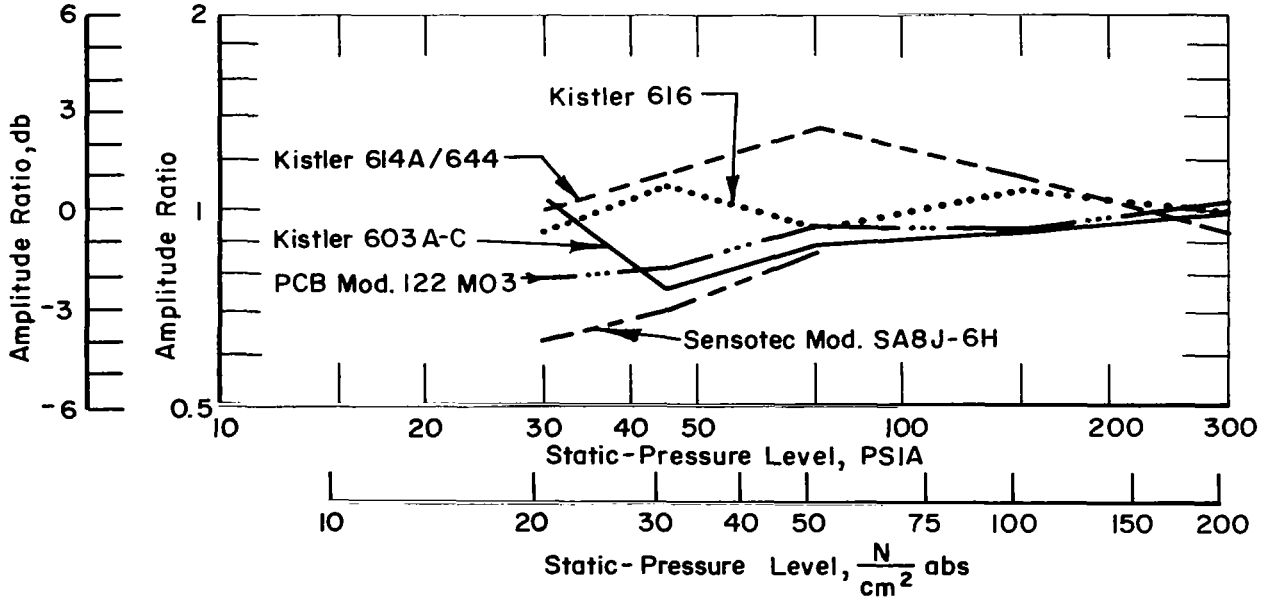

b. Amplitude Ratio vs Frequency, Referenced to Test Kistler 603A

FIGURE 20. AMPLITUDE RATIO vs STATIC-PRESSURE LEVEL FOR ALL TRANSDUCERS